Separate Memory-Enhancing Effects of Reward and Strategic Encoding

Michael S. Cohen, Larry Y. Cheng, Ken A. Paller, and Paul J. Reber

Abstract

■ Memory encoding for important information can be enhanced both by reward anticipation and by intentional strategies. These effects are hypothesized to depend on distinct neural mechanisms, yet prior work has provided only limited evidence for their separability. We aimed to determine whether reward-driven and strategic mechanisms for prioritizing important information are separable, even if they may also interact. We examined the joint operation of both mechanisms using fMRI measures of brain activity. Participants learned abstract visual images in a value-directed recognition paradigm. On each trial, two novel images were presented simultaneously in different screen quadrants, one arbitrarily designated as high point value and one as low value. Immediately after each block of 16 study trials, the corresponding point rewards could be obtained in a test of item recognition and spatial location memory. During encoding trials leading to successful subsequent memory, especially of high-value images, increased activity was observed in dorsal fronto-parietal and lateral occipitotemporal cortex. Furthermore, activity in a network associated with reward was higher during encoding when any image, of high or low value, was subsequently remembered. Functional connectivity between right medial temporal lobe and right ventral tegmental area, measured via psychophysiological interaction, was also greater during successful encoding regardless of value. Strategic control of memory, as indexed by successful prioritization of the high-value image, affected activity in dorsal posterior parietal cortex as well as connectivity between this area and right lateral temporal cortex. These results demonstrate that memory can be strengthened by separate neurocognitive mechanisms for strategic control versus reward-based enhancement of processing. ■

INTRODUCTION

Information designated as important is more likely to be remembered successfully than unimportant information. This is obviously adaptive for memory functioning, and as such, there are likely to be multiple mechanisms within the brain supporting improved memory for important items. In laboratory studies of memory, effects of importance have been studied by manipulating the value of items to be remembered, for example, by offering monetary reward (Shigemune, Tsukiura, Kambara, & Kawashima, 2014; Adcock, Thangavel, Whitfield-Gabrieli, Knutson, & Gabrieli, 2006) or arbitrary point value (Castel, 2008). Novelty (Düzel, Bunzeck, Guitart-Masip, & Düzel, 2010; Lisman & Grace, 2005) or curiosity (Gruber, Gelman, & Ranganath, 2014) may also be useful signals of important information that drive better memory.

One important mechanism by which value can strengthen memory appears to involve the mesolimbic dopamine system, which is broadly associated with reward-motivated behavior in humans and other animals (Schultz, 2016; Berridge, 2007). Functional neuroimaging studies in humans have observed increased activity in reward-sensitive brain regions such as the ventral tegmental area (VTA) and the nucleus accumbens (NAcc) during successful memory encoding when a relatively high reward value is anticipated (Shohamy & Adcock, 2010). Functional connectivity between VTA and hippocampus (Shigemune et al., 2014; Wolosin, Zeithamova, & Preston, 2012; Adcock et al., 2006), or between VTA and parahippocampal cortex (Dillon, Dobbins, & Pizzagalli, 2014), also tends to increase during successful learning of information associated with a high potential reward. Stronger connectivity between VTA and medial temporal lobe (MTL) during a postlearning rest period is additionally associated with stronger memory for high-reward trials (Gruber, Ritchey, Wang, Doss, & Ranganath, 2016).

These findings connect well to studies of the neurobiology of memory in animal models. Dopamine has been observed to play an important role in long-term potentiation in the hippocampus (Lisman, Grace, & Düzel, 2011; Bethus, Tse, & Morris, 2010; O'Carroll & Morris, 2004) indicating a potential mechanism for how key dopamine-producing regions in the midbrain can improve memory. Dopamine is typically released in response to unexpected rewards, anticipation of an upcoming reward, or novelty (Lisman & Grace, 2005; Schultz, 1998). Exposure to novel environments, or introduction of a dopamine agonist, can also lead to memory formation in response to a weak stimulus that would otherwise be forgotten (Li,

Northwestern University

Cullen, Anwyl, & Rowan, 2003). Thus, connections between reward-sensitive regions in the brain and the MTL likely play an important role in the observed strengthening of high-value, important memories.

In addition to reward effects on memory, there is an extensive history of studies showing that utilizing effective strategies during encoding can powerfully enhance memory. Such strategies include using a deep rather than shallow level of processing (Craik & Tulving, 1975; Craik & Lockhart, 1972), generating rather than reading a word (Slamecka & Graf, 1978), and using imagery to produce a richer encoding of an item (Paivio, 1969). People can learn to apply such strategies spontaneously via metacognition (e.g., DeWinstanley & Bjork, 2004). Recent work has also found indications that people learn to selectively engage deep semantic encoding strategies to enhance memory for high-value verbal information (Cohen, Rissman, Hovhannisyan, Castel, & Knowlton, 2017; Cohen, Rissman, Suthana, Castel, & Knowlton, 2014, 2016).

The neural correlates of effective encoding strategies have been extensively examined, with increased activity in left inferior prefrontal regions associated with use of the deep semantic encoding strategies that typically improve memory of meaningful content (e.g., Kirchhoff & Buckner, 2006; Miotto et al., 2006; Kapur et al., 1994). Kirchhoff and Buckner found that visual inspection strategies, associated with increased brain activity in lateral occipitotemporal cortex, are also effective for encoding meaningful picture stimuli. Finally, memory efficacy can be enhanced via strategy-driven, top–down attention effects mediated through the dorsal attention network, particularly dorsal posterior parietal cortex (dPPC). dPPC activity during memory encoding is often associated with successful memory (Uncapher & Wagner, 2009), and the overlap reported by Uncapher, Hutchinson, and Wagner (2011) between activity seen in dPPC during a top–down attention task and successful subsequent memory reinforces the idea that attention plays a role in this process. In addition to increased activity, Uncapher et al. (2011) reported enhanced functional connectivity between posterior parietal and lateral occipitotemporal cortex during successful encoding of stimuli that were within the focus of top–down attention.

We hypothesize that reward and strategic effects on memory reflect two distinct neural processes by which the efficacy of memory encoding in the MTL can be enhanced for high-value information (Cohen et al., 2017). One piece of evidence that these processes are distinct is that that they appear to be differentially affected by healthy aging, as direct effects of reward show degradation with age while selective strategy use largely does not (Geddes, Mattfeld, de los Angeles, Keshavan, & Gabrieli, 2018; Cohen et al., 2016). Cohen et al. (2017) also found that effects of value mediated by verbal strategies are more robust than those observed when no strategy use is reported. On the other hand, the memory-enhancing effects of reward operate under incidental learning conditions in which strategy use is unlikely (e.g., Wittmann et al., 2005), indicating that reward mechanisms do not require top–down conscious control. Effects of reward are also distinct from strategic encoding effects in that the former, in some cases, only emerges with a delay (e.g., Spaniol, Schain, & Bowen, 2014; Murayama & Kuhbandner, 2011), suggesting an influence on consolidation processes.

Reward responses putatively associated with mesolimbic dopamine can also enhance memory even when the association with reward is indirect. For instance, incidental memory for nonrewarded stimuli is enhanced when those items are part of a semantic category that was rewarded earlier (Oyarzún, Packard, de Diego-Balaguer, & Fuentemilla, 2016) or even when an unanticipated association of their semantic category with reward happens minutes after the items were presented (Patil, Murty, Dunsmoor, Phelps, & Davachi, 2017). Temporal contiguity with a reward-predicting stimulus also appears to boost memory. Stimuli incidentally encoded after a positive feedback cue on a previous trial are more likely to be remembered (Mather & Schoeke, 2011). Even when stimuli precede the opportunity to earn rewards, and the reward opportunity is part of an unrelated timing task, incidental encoding is strengthened by rewards (Murayama & Kitagami, 2014).

Although the studies described in the preceding paragraph did not directly measure brain activity, they all suggest that stimulation of the mesolimbic dopamine system is sufficient to enhance encoding of information that is not itself rewarded but that is either conceptually or temporally associated with reward or its anticipation. In this study, low- and high-value items are presented simultaneously. Thus, we predict that activity in the brain's reward system, and connectivity between reward and memory systems, will lead to comparable memory enhancement for both items, even if we assume that these effects are driven by anticipation of the higher reward value. In other words, if incidental learning is strengthened via indirect associations with reward, similar mechanisms could also enhance memory for low-value stimuli presented together with high-value stimuli. Although this is not the only mechanism by which encoding could be enhanced nonselectively on some trials, fMRI data associating reward system activity and VTA–MTL connectivity with successful but nonselective encoding would support this mechanism being a key factor. In contrast, we predict that strategic effects, such as top–down allocation of attention, will specifically enhance memory for high-value items. The stimuli were abstract visual "kaleidoscope" images (randomly generated, deflected, overlaid polygons), reducing the efficacy of semantic encoding strategies that could otherwise overshadow other strategic and reward mechanisms (Han, O'Connor, Eslick, & Dobbins, 2011; Wright et al., 1990). Each image was presented in one of four spatial quadrants (as in Cansino,

Maquet, Dolan, & Rugg, 2002), permitting the assessment of memory context (spatial quadrant of presentation) as well as yes/no recognition memory. The structure of the paradigm was broadly similar to previous studies by Cohen et al. (2014, 2016), in which blocks of stimuli to be studied were followed by immediate tests with points-earned feedback after each block. This study-test cycle structure accentuates the use of encoding strategies and increases attention of the participants to the reward (points) to be gained (Cohen et al., 2017). The activity associated with memory formation was contrasted between successful and unsuccessful memory for high- and low-value items to identify reward-based and strategic effects on memory formation.

METHODS

Participants

Twenty-four young adults enrolled in the study, four of whom were subsequently excluded from all analyses because of technical problems ($n = 1$) or excessive head motion during scanning ($n = 3$). Individuals excluded for excessive head motion had at least three runs with slice-averaged temporal signal-to-noise ratio (mean signal across the time series divided by its standard deviation) < 60, whereas no other participant had more than one such run; poor image quality was confirmed by visual inspection of the data. The 20 included participants (13 women, seven men) ranged in age from 18 to 39 years ($M_{age} = 26.8$ years, $SD = 5.9$). All reported being right-handed and fluent English speakers, with no history of major neurological or psychiatric disorders, no current psychoactive medications, no color blindness, and no other factors that would contraindicate MRI scanning.

All procedures were approved by the Northwestern University institutional review board. Written consent was obtained from all participants. Participants were paid $20/hr; a typical session lasted 3 hr, with 2 hr in the MRI scanner. Participants were recruited via fliers on the Northwestern University Chicago campus and via word of mouth.

Behavioral Procedures and Task Stimuli

Participants were informed that they were participating in a memory study where the stimuli to be remembered were worth differing amounts of points that could be gained by accurate memory at test (points were not related to compensation or any extrinsic reward). Each study trial began with simultaneous presentation of two coin-shaped cues indicating the location and upcoming value of a stimulus on a 2 × 2 grid. High-value stimuli were worth 10 or 12 points, and low-value stimuli were rewarded with 2 or 3 points (Figure 1). Stimuli to be remembered were abstract visual "kaleidoscope" images generated using an algorithm initially described by Miyashita, Higuchi, Sakai, and Masui (1991) for creating novel, arbitrary, visual images by random deflection of colored polygons. On each trial, the value information was presented for 2.5 sec, and after a 1.0-sec blank delay, the two memory stimuli were presented on-screen simultaneously for 5 sec, followed by another 0.5-sec delay. After studying the visual stimuli, participants completed a baseline task consisting of a left/right (< or >) arrow direction judgment for 2–8 sec (times selected to optimize subsequent trial deconvolution), with each arrow appearing for 0.8 sec each (plus 0.2-sec ISI). An additional 1.0-sec ITI followed the final arrow. The arrows task was intended to keep participants' attention focused on a low-level task during the baseline period to maximize effectiveness of contrasts among trial types (Stark & Squire, 2001). At the end of each scanning run of the encoding task, on-screen feedback was provided about accuracy on the arrows task for that list to encourage compliance with the baseline task.

Visual stimuli to be remembered were presented in blocks of 16 trials containing two stimuli (one high value, one low value) in each trial. Stimuli were presented twice each, always in the same quadrant and paired with the same value, but paired with different images on each presentation. Re-pairing was intended to prevent creation of item–item associations that could interfere with prioritization of high-value items. Each scanning run included 16 unique stimuli. Assignment of specific images to values was counterbalanced across participants. Across six runs, 96 unique kaleidoscope images were studied in the scanner during the encoding phase.

After each study run, participants completed a memory test for the stimuli presented in the prior list. The memory test was used to post hoc sort the successful and unsuccessful encoding trials. It was administered in the scanner, and fMRI data were collected; these data will be reported in a separate publication. The test included the 16 images that had appeared on the preceding study list and eight dissimilar foil images, presented in randomized order (see Figure 1). During the 4-sec presentation, participants were required to judge both whether the stimulus was old or new and, if old, which quadrant it had appeared in during study. Participants were instructed they needed to remember the location of old images to earn the stated point value from the study phase. Items that were correctly identified as old but in the wrong quadrant and correctly identified new items were both awarded 1 point. Confidence judgments were provided after the memory test response and a 1-sec delay but were not used in the analysis of the imaging data collected during study. For "old" responses, a 3-point confidence rating was provided: 1 = *confident in both the item being "old" and in its location*, 2 = *confident that the item was "old" but guessing about location*, or 3 = *guessing on both*. For "new" responses, participants were asked whether that response was 1 = *confident* or 2 = *guess*. Confidence judgments were also followed by a jittered fixation interval, ranging in length from 2 to 8 sec, optimized for trial deconvolution.

Figure 1. Task figure. Neuroimaging analysis is focused on a 9-sec time window for the study (encoding) task, which includes the value cue (2.5 sec), a 1-sec fixed interval with a blank grid, image display (5 sec), and another blank grid interval (0.5 sec). The arrow judgment active baseline period follows, with jittered duration (3–9 sec). Each study trial includes one high-value (10- or 12-point) cue and one low-value (2- or 3-point) value cue. After 16 encoding trials, participants see a yes-no/quadrant recognition test on the preceding set of items. Item and quadrant memory judgments are made simultaneously, within a 4-sec time window. After a short fixation interval, participants respond to a confidence prompt, followed by a fixation baseline with jittered duration. After each test, feedback is given to indicate the point total for all items correctly recalled on that test. This procedure repeats six times.
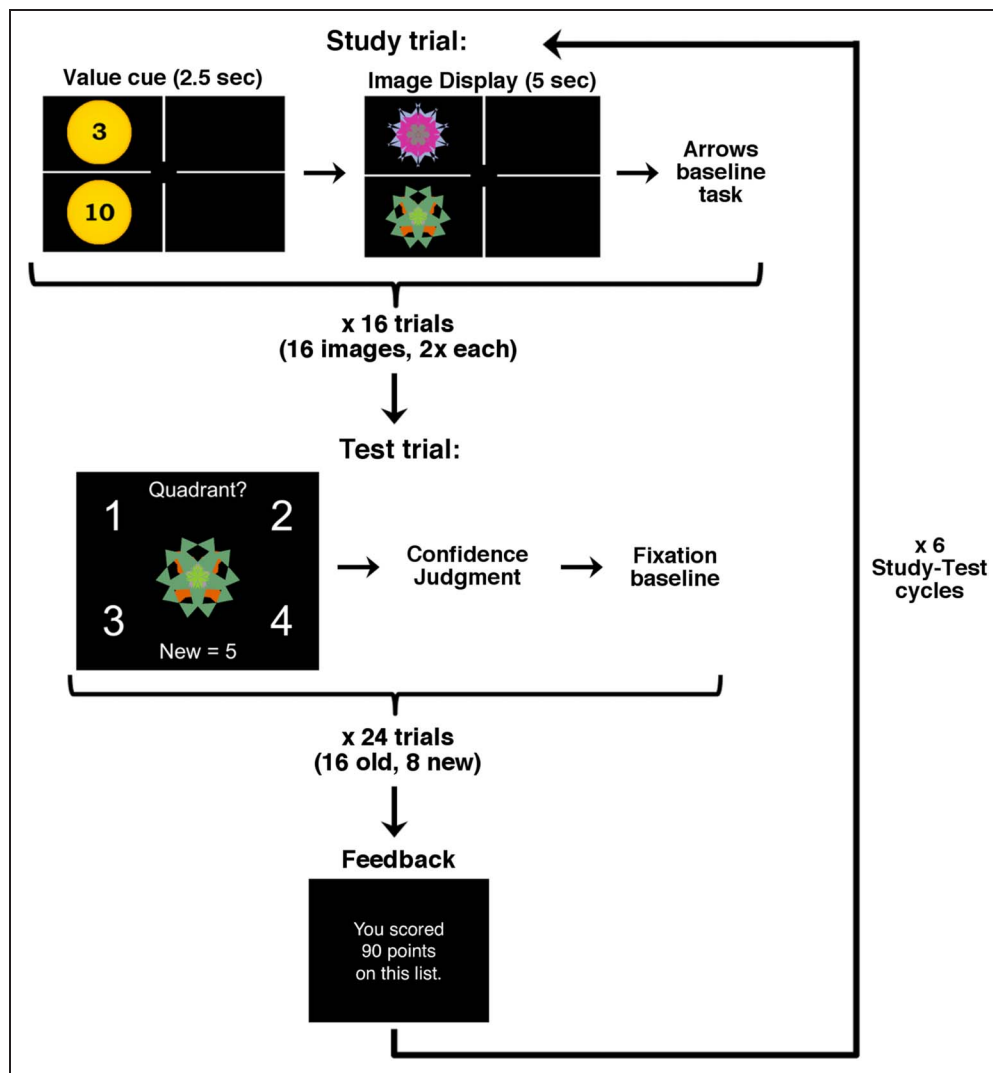
To familiarize participants with the study/test protocol structure before scanning, participants were given an initial practice phase consisting of four encoding trials, with eight images presented once each followed by a short practice test phase in which nine images (six old, three new) were presented. Participants then completed one full-length encoding list and one full test list. Prior work has shown that extended practice leads to more consistent strategy use later, that is, in the scanner (Cohen et al., 2016; Castel, 2008). Neuroimaging data were then collected from six full study lists, each followed by a test. After all six study-test cycles, an additional forced-choice recognition test for all study stimuli was administered (reported separately). After the fMRI session, participants were debriefed to gain some insight about the strategies that participants used during learning.

Scanning Procedure

T2*-weighted echo-planar (EPI) images sensitive to BOLD contrast were collected using a 3-T Siemens Prisma MRI scanner at the Northwestern Center for Translational Imaging. For the study task, each run lasted 4 min 28 sec, and 130 whole-brain volumes were collected (after four discarded volumes at the beginning). Each functional volume contained 56 interleaved slices, repetition time (TR) = 2000 msec, echo time = 25 msec, flip angle = 80°, slice thickness = 2.0 mm, in-plane resolution = 2.0 × 2.0 mm, matrix = 104 × 98, field of view = 208 mm × 192 mm, and no gap between slices. We also collected a high-resolution EPI-navigated structural scan, with the following parameters: TR = 2170 msec, echo time = 1.69 msec, flip angle = 7°, 1-mm³ voxels, field of view = 176 mm × 256 mm × 256 mm, with GRAPPA acceleration. To minimize head movement during scanning, we placed cushions between the participant's head and the coil. Stimuli were presented using PsychoPy v1.82 software (Peirce, 2007), and images were shown via a high-resolution MRI-compatible monitor (Nordic Neuro Lab), visible via a mirror placed on top of the head coil. Responses were collected using a five-button fiber optic input device, connected to a response box in the scanner

control room (MRA, Inc.) running a Cedrus RB-834 circuit board. The response pad interfaced with PsychoPy using the Cedrus PyXID driver library.

fMRI Data Analysis

Preprocessing

Initial preprocessing was run via the Northwestern Neuroimaging Data Archive (NUNDA). High-resolution structural images were filtered using N4 bias correction (Tustison et al., 2010) and filtered using a nonlocal means filter (Tristán-Vega, García-Perez, Aja-Fernández, & Westin, 2012). Further preprocessing was carried out using FEAT v6.00 (fMRI Expert Analysis Tool), as implemented in FMRIB Software Library (FSL) v5.0.9 (www.fmrib.ox.ac.uk/fsl). Head motion was corrected using MCFLIRT (FMRIB's motion correction linear image registration tool; Jenkinson, Bannister, Brady, & Smith, 2002), and nonbrain tissue was removed using BET (Brain Extraction Tool; Smith, 2002). BOLD data were grand-mean intensity normalized within each run using a multiplicative scaling factor and smoothed with a 5-mm Gaussian kernel (FWHM). A high-pass filter was used to remove low-frequency noise using a Gaussian-weighted least-squares straight-line fitting with a sigma of 50 sec. Temporal autocorrelation was corrected for using prewhitening as implemented by FILM (FMRIB's Improved Linear Model; Woolrich, Ripley, Brady, & Smith, 2001). Functional images were registered to a high-resolution structural scan using FLIRT (FMRIB's Linear Image Registration Tool) linear registration. Registration from the high-resolution structural scan to standard Montreal Neurological Institute (MNI) space was further refined using FNIRT (FMRIB's Nonlinear Image Registration Tool).

Univariate Analysis

We sorted study trials by memory success of the two items, with four possible trial types: both items correct (H+L+), high-value correct/low-value incorrect (H+L−), low-value correct/high-value incorrect (H−L+), and neither item correct (H−L−). In addition, trials in the first half of each run (first presentation) were modeled separately from trials in the second half of the run (second presentation). Thus, there were up to eight regressors in each first-level analysis. Preliminary analyses found no differences in brain activity between the first and second presentations of each item, so all reported analyses average across this factor. Each trial was modeled as the 9-sec period from when the value cues appeared until the arrows task began, convolved with a double-gamma hemodynamic response function (HRF). Temporal derivatives were also included in the model for each regressor, to account for minor deviations between the modeled and actual HRFs. Motion regressors, and regressors coding for any motion outlier TRs, were also included in the model

as covariates of no interest. Censoring motion outlier volumes eliminates more motion-related noise than only modeling motion regressors (Siegel et al., 2014). Benefits of using both methods simultaneously are less clear; Siegel et al. indicate that reduced statistical power is possible, but we assume that this approach errs, if at all, on the conservative side. Motion outlier volumes were defined using default settings in *fsl_motion_outliers*: Volumes exceeding a threshold of the 75th percentile + 1.5 × the interquartile range, for root mean square intensity difference relative to the middle volume of the run, were regressed out. The first-level general linear model analysis was carried out separately for each run. A second-level fixed effects analysis combined parameter estimates across all six runs and created a set of linear contrasts for comparisons of interest (equal weights were used for parameter estimates from the first and second halves of each run). Second-level analysis results were used as inputs to subsequent whole-brain and ROI analyses at the group level. To be included in the group analysis, participants were required to have a minimum of five trials for each considered trial type. Three individuals were excluded from all group-level fMRI contrasts comparing successful memory trials to H−L− trials (one participant with fewer than five H−L− trials and two participants with fewer than five H+L+ trials), yielding 17 individuals included in those analyses. Mean trial counts for these 17 participants were as follows: H+L+, 26.8; H+L−, 26.4; H−L+, 15.9; H−L−, 25.9. Direct contrasts between H+L− trials and H−L+ trials included all 20 participants (mean trial counts: H+L−, 26.3; H−L+, 14.9).

For the third-level whole-brain analysis across participants, we used the FLAME Stage 1 and Stage 2 mixed-effect model in FSL, with automatic outlier detection (Woolrich, 2008). Clusters were determined using a voxel-level threshold of $z > 3.1$, with a cluster-corrected significance level of $p < .05$. Cortical surface renderings were created using Caret v5.65 (brainvis.wustl.edu; Van Essen et al., 2001) on the inflated Conte69 atlas in FNIRT space (Van Essen, Glasser, Dierker, Harwell, & Coalson, 2012), with FSL activation maps transformed from volume to surface space using Caret's interpolated voxel algorithm. Activation peaks noted in the tables were a subset of the local maxima generated for each contrast by FSL's *cluster* command, with a minimum distance of 10 mm between peaks. Labels were determined using the FSL Harvard-Oxford probabilistic structural atlas (fsl.fmrib.ox.ac.uk/fsl/fslwiki/Atlases) and other relevant brain maps (e.g., Yarkoni, Poldrack, Nichols, Van Essen, & Wager, 2011; Eickhoff et al., 2005; Talairach & Tournoux, 1988; Brodmann, 1909), and redundant peaks were eliminated.

Connectivity Analyses

Task-dependent connectivity between brain regions was assessed using a psychophysiological interaction (PPI) analysis (McLaren, Ries, Xu, & Johnson, 2012; Friston

et al., 1997). Seed region time series was extracted in native space from nuisance analysis residuals, after preprocessing raw data and regressing out six motion parameters in FEAT. Inverted FLIRT and FNIRT registration transforms were applied to standard-space ROIs of targeted regions, and the time series from each targeted voxel was averaged across the ROI. PPI analysis regressors were constructed using AFNI (Cox, 1996).[1] The seed region time series was initially up-sampled by a factor of 20, and the neural impulse responses were estimated by deconvolving a gamma function HRF from the time series. The following regression options were used for this deconvolution: lasso regression with lambda = −6, penalty factor on the signal estimate and its first and second derivatives, and −2 penalty weighting. Raw psychological regressors were each multiplied by the deconvolved seed region time series to produce a set of PPI regressors, which were then convolved with a gamma HRF. The physiological regressor was generated by reconvolving the deconvolved seed region time series with a gamma HRF, following Di, Reynolds, and Biswal (2017). Psychological regressors were also convolved with a gamma HRF. Finally, all regressors were downsampled by a factor of 20 and then input back into FEAT as part of a new first-level analysis. Input data were the nuisance analysis residuals, with a value of 10,000 units added to all voxels. No additional preprocessing was done. The first-level FEAT model for each run included psychological and PPI regressors for each condition, the physiological regressor, and six dummy regressors accounting for degrees of freedom used by motion parameters in the nuisance analysis. The temporal derivatives of the psychological regressors were computed by FEAT and included in the model, and temporal filtering was applied to the psychological regressors. In addition, motion outlier TRs were regressed out using nuisance regressors. Data from all six encoding runs were combined in a second-level fixed effects analysis, where contrasts of interest were computed. These second-level contrast estimates then served as inputs to the final group-level analysis, which was run using the FLAME1 and FLAME2 mixed effects model with automatic outlier detection. For PPI analyses, a voxel threshold of $z > 2.3$ was used, with cluster threshold added to reach $p < .05$. This lower voxel threshold reflects the reduced statistical power caused by increased collinearity in PPI relative to univariate analyses but does elevate false-positive risk (Eklund, Nichols, & Knutsson, 2016).

For the PPI analysis examining connectivity with MTL, the seed region was defined as an 8-mm-radius sphere centered on the peak voxel in right MTL from the meta-analysis by Kim (2011). The laterality of our MTL seed is justified by neuropsychological work showing laterality effects for visual versus verbal stimuli, with memory for abstract visual stimuli depending primarily on right MTL (e.g., Jones-Gotman, 1986; Milner, 1958). Increases in MTL–VTA functional connectivity related to reward anticipation during encoding are often lateralized to right MTL

as well, whether for scenes (Adcock et al., 2006), object drawings (Dillon et al., 2014), or even words (Shigemune et al., 2014). The right MTL seed region was further masked by an MTL anatomical ROI, defined as voxels in the FSL Harvard-Oxford structural atlas having a most likely label of either parahippocampal gyrus or hippocampus. Because we were specifically interested in functional connectivity between MTL and VTA, we applied a prethreshold anatomical mask in this analysis to limit the search space to VTA. This was defined as voxels with at least a 25% chance of being in VTA according to a probabilistic midbrain atlas (Murty et al., 2014). For the PPI analysis examining parietal connectivity, the seed region was defined as the full clusters in bilateral posterior parietal cortex emerging from the univariate H+L− > H−L+ contrast. The target search space was restricted to inferior portions of lateral temporal and lateral occipital cortex, to enhance statistical power to detect a connectivity effect analogous to that reported by Uncapher et al. (2011). This target region was defined using the FSL Harvard-Oxford atlas, including all voxels with at least a 1% chance of being in either the temporo-occipital part of the inferior temporal gyrus or the inferior division of the lateral occipital cortex.

ROI Analyses

To target the reward system, hypothesized to be important for value-based memory, an anatomical ROI was defined from an automated meta-analysis of published results in Neurosynth (Yarkoni et al., 2011). Relevant studies were selected using the "topics" feature, in which studies related to each of 100 topics were grouped using latent Dirichlet allocation (Poldrack et al., 2012). The reward ROI (Figure 3A) was defined using a set of 532 studies associated with keywords such as "reward," "motivation," "incentive," and "mesolimbic" and consisted mainly of the NAcc and VTA as well as small clusters in ventromedial PFC. The default "reverse inference" map (areas where activity is selectively associated and potentially diagnostic of reward processing) provided by Neurosynth (based on a false-discovery-rate-corrected $p < .01$ threshold) was further restricted by an additional voxelwise threshold of $z > 5.20$, corresponding to $p < .0000001$, one-tailed, yielding a map with 3,641 voxels. The z statistic for each voxel was computed via a χ^2 test of independence examining whether the proportion of studies in which the voxel is active differs for studies associated with the topic of interest, compared with all other studies in the Neurosynth database. For a control ROI comparison, a "default mode" network ROI was defined using the same technique, identifying 566 articles associated with such terms as "default," "dmn," and "deactivation," yielding a map with 4,120 voxels. Assessment of activity was based on averaged parameter estimate (COPE) values across all voxels within each ROI, for each participant, for the second-level FEAT contrasts between

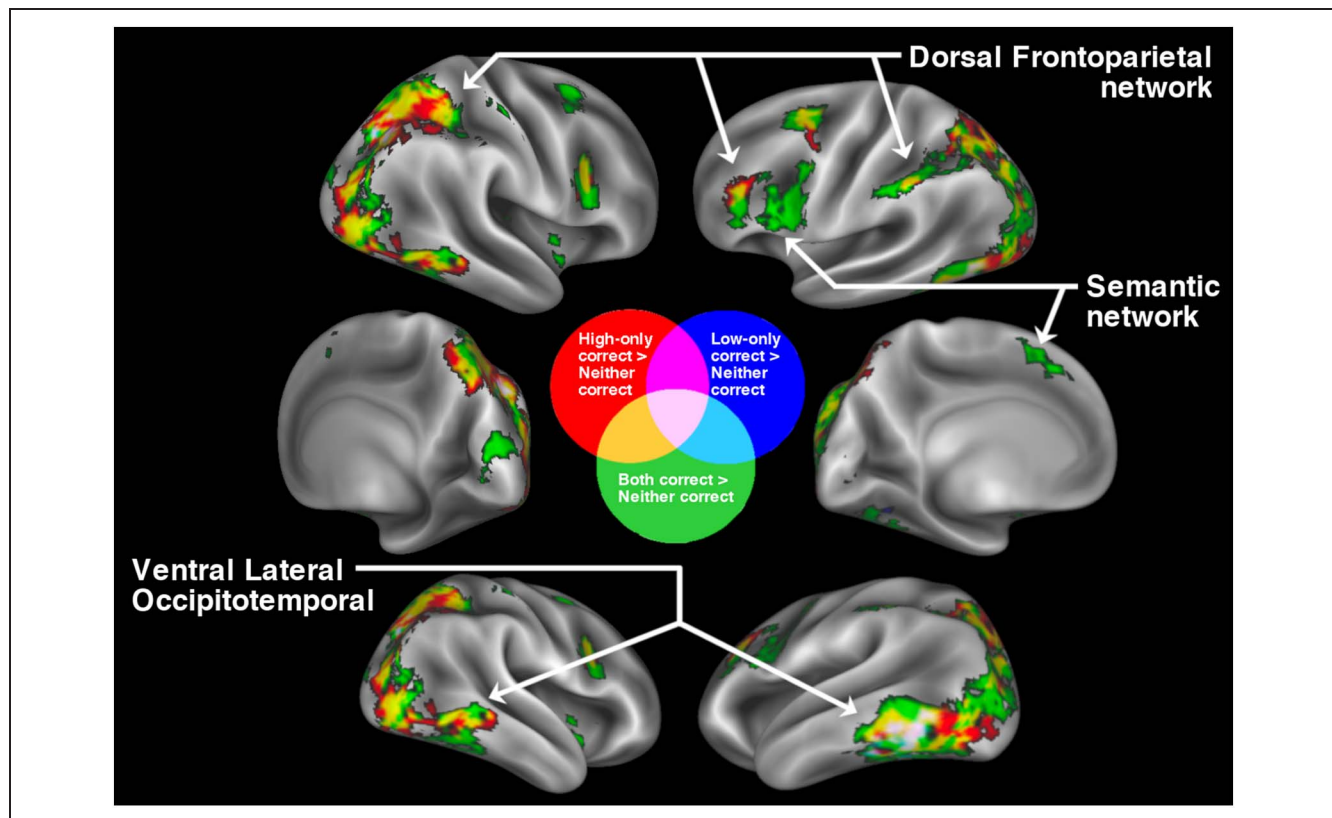successful memory (H+L+, H+L−, and/or H−L+) and memory failure (H−L−).

RESULTS

Behavioral Results

Participants exhibited better memory for high-value than low-value stimuli on the item and source/quadrant memory test (high-value items: $M = 55.2\%$ correct, $SE = 4.0\%$; low-value items: $M = 43.4\%$ correct, $SE = 4.4\%$), $t(19) = 4.41$, $p < .001$, $d = 0.99$. The rate at which old items were correctly judged as old regardless of the accuracy of the quadrant response (i.e., item hit rate) was also higher for high-value items ($M = 88.9\%$ correct, $SE = 2.5\%$) than for low-value items ($M = 81.6\%$ correct, $SE = 4.0\%$), $t(19) = 2.95$, $p = .008$, $d = .66$. Both high- and low-value items were judged old at a higher rate than new items on the test (i.e., the false alarm rate, $M = 37.7\%$, $SE = 4.0\%$), $t(19) = 13.08$, $p < .001$, $d = 2.93$ (high-value items), and $t(19) = 10.02$, $p < .001$, $d = 2.24$ (low-value items). Memory within

each value grouping (i.e., 2 vs. 3 points within low-value items and 10 vs. 12 points within high-value items) did not differ for either memory measure, all $|t|$s < 1.23, all ps $> .233$.

Confidence judgments were well aligned with response accuracy. Across images judged as old, the proportion for which participants reported being confident about both item and location was greater for trials in which both aspects were correctly remembered ($M = 65.4\%$, $SE = 4.1\%$) than for trials in which only the item judgment was accurate ($M = 22.0\%$, $SE = 3.6\%$), $t(19) = 12.11$, $p < .001$, $d = 2.71$, and was still lower for foils ($M = 9.5\%$, $SE = 2.7\%$), $t(19) = 3.72$, $p = .001$, $d = .83$. The proportion of images for which participants reported being confident only in the item recognition judgment was highest when only the item was correct ($M = 56.5\%$, $SE = 3.8\%$), was lower for foils ($M = 41.6\%$, $SE = 5.7\%$), $t(19) = 3.55$, $p = .002$, $d = .79$, and was still lower when both item and quadrant were correct ($M = 24.6\%$, $SE = 2.9\%$), $t(19) = 2.63$, $p = .016$, $d = .59$. Finally, judgments of an image as new were more likely to be made

Figure 2. Subsequent memory effects: increased activity for any successful memory (H+L+, H+L−, and H−L+) compared with unsuccessful memory (H−L−). Subsequent memory effects shown here largely echo those observed from other studies, despite atypical features of our encoding paradigm such as simultaneous presentation of high- and low-value items and the use of novel abstract images as memoranda. Specifically, trials for which only the high-value item was later recalled (H+L−, in red) and trials for which both items were later recalled (H+L+, in green) show activation bilaterally in a dorsal frontoparietal network (typically associated with working memory and controlled attention) and ventral lateral occipitotemporal regions (typically associated with shape and color perception) as well as FEFs (associated with spatial attention). Many of these activations overlap (shown in yellow). Trials for which only the low-value item was later recalled (H−L+, in blue) show activity in a similar set of regions, although more constrained, with reliable clusters only in left lateral occipitotemporal cortex and right intraparietal sulcus. (These clusters overlap with activity in other conditions and thus are shown in white/gray.). H+L+ trials also show activity in a network of left-hemisphere regions typically associated with semantic processing.

Table 1. Cluster Peaks and Relevant Subpeaks for Univariate Subsequent Memory Contrasts

Cluster Number	Region	BA	Peak MNI Coordinates			Z_{max}	Cluster Size (Voxels)
			x	y	z		
Both correct (H+L+) > neither correct (H−L−)							
1	L supramarginal gyrus	40	−44	−44	50	5.72	4079
	L extrastriate visual cortex (V5/MT)	19	−46	−74	−4	5.39	
	L lateral extrastriate visual cortex	18/19	−36	−90	8	5.10	
	L fusiform gyrus	19/37	−40	−66	−8	5.08	
	L lateral/dorsal extrastriate visual cortex	19	−38	−82	18	4.99	
	L dorsal extrastriate visual cortex (V2/V3)	18/19	−18	−90	22	4.80	
	L superior parietal lobule	7	−28	−76	48	4.79	
	L ventral extrastriate visual cortex (V4)	19	−36	−76	−8	4.62	
	L inferior temporal gyrus	20/37	−46	−58	−14	4.57	
	L intraparietal sulcus	40	−46	−38	42	4.14	
	L cerebellum	–	−12	−68	−14	3.80	
	L primary visual cortex (V1)	17	−12	−90	6	3.72	
2	R intraparietal sulcus	7	32	−74	38	5.60	2579
	R extrastriate visual cortex (V5/MT)	19	46	−80	6	5.16	
	R lateral extrastriate visual cortex	19	38	−84	12	5.15	
	R superior parietal lobule/intraparietal sulcus	7	32	−50	56	4.97	
	R superior parietal lobule	7	18	−66	58	4.79	
	R primary/secondary visual cortex (V1/V2)	17/18	8	−92	12	4.58	
	R ventral extrastriate visual cortex (V3/V4)	19	38	−76	−4	4.42	
	R supramarginal gyrus	40	46	−40	60	4.37	
	R precuneus	7	10	−74	54	4.28	
	R dorsal extrastriate visual cortex (V2/V3)	18	18	−90	14	4.19	
	R somatosensory cortex	2	56	−26	58	4.10	
3	L inferior frontal gyrus, pars opercularis	44	−40	8	26	5.18	768
	L premotor cortex	6	−48	6	20	4.63	
	L dorsolateral PFC	9	−52	28	28	4.57	
	L inferior frontal gyrus, pars triangularis	45	−40	30	18	4.26	
4	R middle temporal gyrus	37	60	−58	−8	4.72	641
	R inferior temporal gyrus	37	46	−50	−12	4.62	
	R fusiform gyrus	37	38	−58	−12	4.26	
5	R putamen	–	24	14	−2	4.94	519
	R amygdala	–	28	0	−10	4.21	
	R insula	13	38	2	−6	4.17	
	R striatum	–	16	2	0	4.12	
	R caudate	–	8	14	2	3.98	
6	L putamen	–	−20	14	8	4.58	484
7	L FEFs/middle frontal gyrus	6	−24	4	50	4.46	257

Table 1. (*continued*)

Cluster Number	Region	BA	Peak MNI Coordinates			Z_{max}	Cluster Size (Voxels)
			x	y	z		
8	R FEFs/middle frontal gyrus	6	24	8	50	4.31	244
9	R inferior frontal gyrus, pars opercularis	44	46	10	22	4.62	230
10	L paracingulate gyrus	32	−8	28	40	4.34	215
	L pre-SMA	6/8	−2	10	54	4.31	
11	R thalamus	–	22	−28	8	4.18	89
	R putamen	–	30	−20	6	4.17	

High value only correct (H+L−) > neither correct (H−L−)

Cluster Number	Region	BA	Peak MNI Coordinates			Z_{max}	Cluster Size (Voxels)
1	R superior parietal lobule	7	30	−72	44	4.80	3022
	R ventral extrastriate visual cortex (V5/MT)	19	50	−62	−10	4.70	
	R intraparietal sulcus	7	34	−48	50	4.59	
	R middle/inferior temporal gyrus	20/37	44	−52	−6	4.41	
	R precuneus	7	8	−72	56	4.40	
	R ventral extrastriate visual cortex (V3/V4)	18	26	−88	−4	4.37	
	R dorsal extrastriate visual cortex (V2/V3)	18	30	−84	8	4.33	
	R fusiform gyrus	19	28	−76	−18	4.18	
	R supramarginal gyrus	40	46	−42	54	4.12	
	R angular gyrus	39	38	−54	40	3.76	
2	L ventral extrastriate visual cortex (V4)	19	−44	−80	−6	5.41	2462
	L dorsal extrastriate visual cortex (V3)	19	−28	−90	26	4.80	
	L inferior temporal/occipital cortex	37	−50	−70	−10	4.61	
	L intraparietal sulcus	7	−28	−76	34	4.56	
	L supramarginal gyrus	40	−48	−38	46	4.56	
	L fusiform gyrus	19/37	−36	−80	−16	4.48	
	L superior parietal lobule	7	−16	−66	46	4.21	
	L extrastriate visual cortex (V5/MT)	19	−42	−82	10	4.21	
	L lateral extrastriate visual cortex	18	−34	−94	8	3.57	
	L precuneus	7	−8	−74	50	3.45	
3	L dorsolateral pFC	9/46	−42	28	30	4.48	280
4	L premotor cortex/FEFs	6	−26	0	52	4.22	139
5	R inferior frontal gyrus, pars opercularis	44	34	6	24	4.18	112

Low value only correct (H−L+) > neither correct (H−L−)

Cluster Number	Region	BA	Peak MNI Coordinates			Z_{max}	Cluster Size (Voxels)
1	L extrastriate visual cortex (V5/MT)	19	−42	−64	−4	4.42	323
	L fusiform gyrus	20/37	−40	−44	−16	4.11	
	L inferior temporal gyrus	37	−48	−64	−14	4.05	
2	R intraparietal sulcus	7	30	−64	36	4.19	116
	R superior parietal lobule	7	28	−68	50	3.46	

Figure 3. Increased activity in the mesolimbic dopamine reward system during study, and increased functional connectivity between MTL and VTA during study, is associated with subsequent memory success. (A) Extent of reward network ROI derived from Neurosynth automated meta-analysis. (B) Parameter estimates for evoked activity averaged across all voxels within the ROI. Brain activity in trials associated with successful memory was greater than in trials with neither item recalled (H−L−); this effect was apparent whether both items (H+L+), the high-value item only (H+L−), or the low-value item only (H−L+) was recalled. Error bars represent ±1 *SE*. (C) VTA cluster in which connectivity with the right (R) MTL seed was stronger when any item was recalled later (H+L+, H+L−, H−L+), relative to trials in which neither item was recalled later (H−L−). (D) The degree to which R MTL–VTA connectivity was higher when any item was recalled later correlates with the combined recall score for high-value and low-value items.
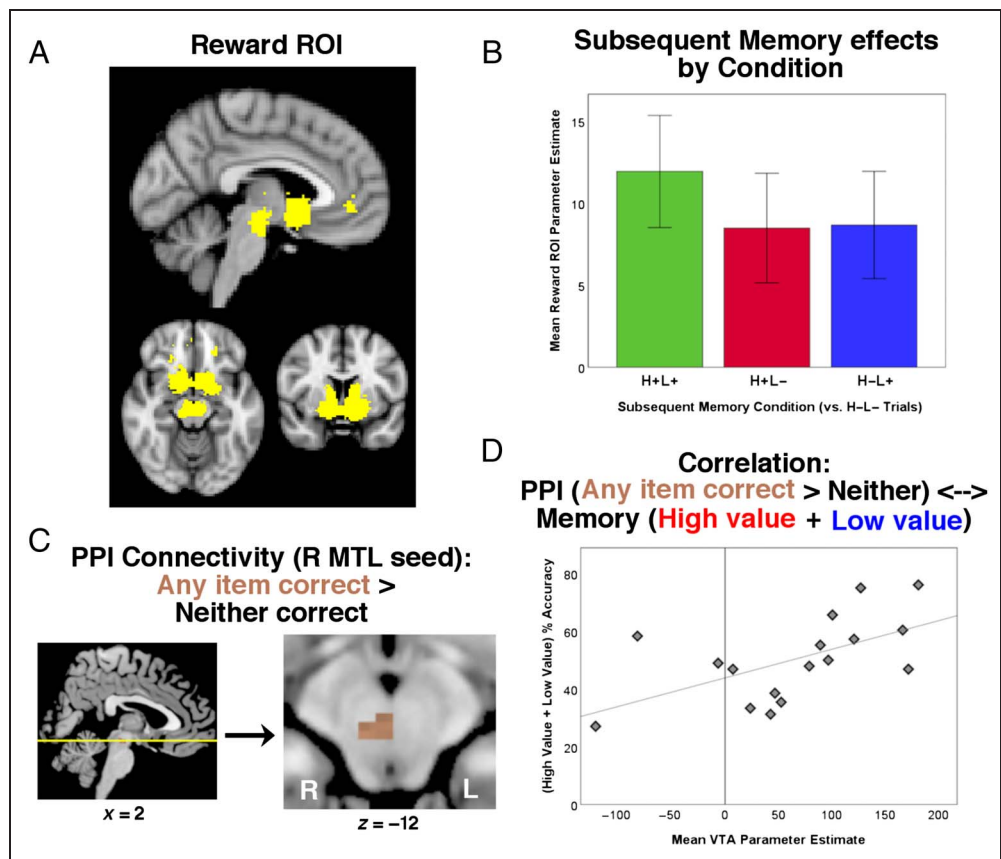
with confidence when the item was in fact a foil ($M = 58.6\%$, $SE = 6.0\%$) than when it was actually old ($M = 42.6\%$, $SE = 6.4\%$), $t(17) = 3.52$, $p = .003$, $d = .83$; two participants were excluded from this comparison because they had no missed old items with valid confidence responses. Because confidence was highly correlated with accuracy, it was not possible to separately incorporate confidence judgment accuracy into post hoc trial sorting.

On the poststudy debriefing, participants described their primary encoding strategy as either associating images with a conceptual meaning or words ($n = 11$), strategies related to perceptual features of the shapes within each image ($n =$ 8), or reported not using any particular strategy ($n = 1$). In addition, some participants described explicit efforts to focus more on high-value items ($n = 16$), whereas others reported not using such efforts ($n = 4$).

Brain Regions Related to Successful Encoding

A widespread set of brain networks exhibited greater activity for successful memory encoding than for stimuli that were not later successfully remembered (Figure 2; Table 1). Across all types of successful encoding trials, we found bilateral activity in frontoparietal regions such as

Table 2. Cluster Peaks in VTA for PPI Analysis with Right MTL Seed Region, Showing All Contrasts with Significant Condition-Specific Enhancement in Connectivity with this Seed Region

Contrast	Peak MNI Coordinates			Z_{max}	Cluster Size (Voxels)
	x	*y*	*z*		
Both correct (H+L+) > neither correct (H−L−)	4	−22	−12	3.12	32
Low value correct (H−L+) > neither correct (H−L−)	−2	−22	−8	3.34	54
High value correct (H+L−) > neither correct (H−L−) (*p* < .10)	6	−20	−12	2.86	12
Any item correct (H+L+, H+L−, H−L+) > neither correct (H−L−)	6	−22	−12	2.90	24
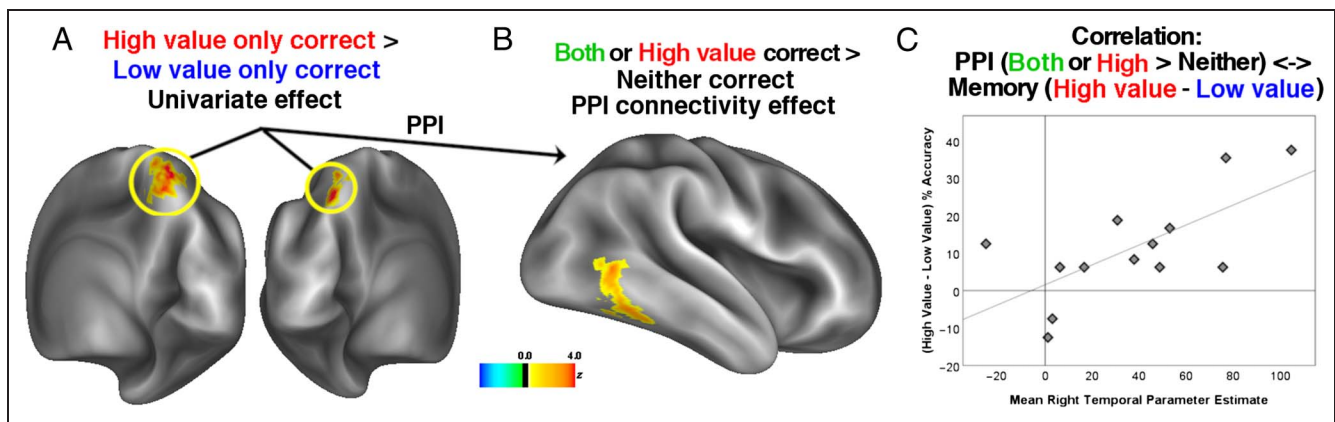
Figure 4. Increased medial parietal activity during a trial and individual differences in connectivity between medial parietal and lateral occipital complex regions when high-value items are successfully encoded are associated with selective memory for high-value items. Analyses are restricted to individuals reporting use of explicit strategies. (A) Bilateral medial dPPC is more active during encoding trials for which the high-value item was later recalled (H+L−), relative to trials for which only the low-value item was recalled (H−L+), suggesting that activity in this brain region leads to selectivity during encoding. (B) Enhanced task-dependent connectivity to right posterior inferior temporal cortex during trials with either the high-value item correct (H+L−) or both items correct (H+L+) relative to trials with neither item correct (H−L−), identified by PPI analysis using as seed regions the bilateral clusters from the analysis shown in A. (C) Greater parietal–temporal connectivity during trials in which the high-value item or both items were successfully learned is correlated with global memory selectivity across participants. This result supports our interpretation that the connectivity effect shown in B reflects top–down allocation of attention toward learning high-value items.

dorsolateral PFC and intraparietal sulcus, typically related to attentional control and working memory. There were also strong clusters of activation in ventral occipitotemporal regions typically associated with object and shape perception, such as lateral occipital complex, as well as some activation in more dorsal portions of lateral occipital cortex. Additional activity in more superior aspects of PFC, in or near the FEFs, was likely a function of the spatial nature of this memory task. Finally, when both items were successfully recalled, we found activity in brain regions typically associated with semantic encoding, such as left inferior prefrontal and left pre-SMA. Brain activity was thus consistent with prior subsequent memory findings (cf. Kim, 2011).

Reward System Activity and MTL–VTA Connectivity

Within the targeted reward system ROI (Figure 3A; see above for selection details), significantly increased activity was observed for successful encoding trials compared with unsuccessful memory (Figure 3B). This effect was observed when both items were recalled (H+L+), $t(16) = 3.49, p = .003, d = .85$, when only the high-value item was recalled (H+L−), $t(16) = 2.53, p = .022, d = .61$, and when only the low-value item was recalled (H−L+), $t(16) = 2.65, p = .017, d = .64$ (Figure 3B). A one-way repeated-measures ANOVA showed no difference between these three conditions, $F(2, 32) < 1, \eta_p^2 = .02$. Even when individuals who reported not being explicitly selective are removed from the analysis, BOLD signal in the reward network did not differ between the three successful memory conditions, $F(2, 24) < 1, \eta_p^2 = .06$. Thus, evoked activity in the reward system appears to be associated with successful memory formation regardless of the value of information remembered.

To examine the selectivity of the successful memory effect to the reward ROI (and the areas shown in Figure 2), a parallel ROI analysis of the default mode network was carried out. The default mode network showed no evidence of differential activity during any type of successful encoding trial, relative to unsuccessful encoding, all $|t|s < 1.44$.

We then examined functional connectivity between a seed region in right MTL and VTA during successful versus unsuccessful encoding. A focus on right MTL is consistent with expectations from prior studies (see Methods). Initial analyses showed significantly greater connectivity between right MTL and VTA for the H+L+ and H−L+ conditions and marginally greater connectivity for the H+L− condition (cluster: $.05 < p < .10$), relative to H−L− trials (Table 2). These findings, and the observation (see Figure 3B) that univariate reward system activity was elevated to a similar degree with any successful encoding, motivated a combined second-level FEAT contrast combining together H+L+, H+L−, and H−L+ (any successful memory) trials, relative to H−L− trials (Figure 3C; see also Table 2). Parameter estimates within this cluster do not differ between the H+L+, H+L−, and H−L− conditions, $F(2, 32) < 1, \eta_p^2 = .05$. The degree to which memory success affected right MTL–VTA connectivity in the combined analysis correlated reliably with performance on the memory test, measured as mean proportion recall for all items (high value and low value), $r = .58, p = .015$ (Figure 3D). This relationship remained reliable after removal of the two outlier participants with substantially negative PPI values, $r = .67, p = .007$.

Selectivity Analyses

None of the preceding analyses identified neural activity associated with the behavioral result showing better

Table 3. Cluster Peaks and Relevant Subpeaks for High-Only Correct (H+L−) > Low-Only Correct (H−L+) Univariate Contrast

| Cluster Number | Region | BA | Peak MNI Coordinates | | | Z_{max} | Cluster Size (Voxels) |
			x	y	z		
1	R superior parietal lobule	7	14	−64	60	4.69	245
	R precuneus	7	4	−54	44	3.88	
	L precuneus	7	−2	−60	54	3.72	
2	L inferior frontal gyrus, pars opercularis	44	−60	16	12	4.27	190
	L dorsolateral PFC	9	−54	24	26	4.24	
	L frontal pole	10/46	−50	46	0	4.12	
	L inferior frontal gyrus, pars triangularis	45	−54	32	12	4.04	
3	L superior parietal lobule	7	−16	−70	52	4.86	189
	L precuneus	7	−8	−66	64	4.13	

memory for high-value images. To strengthen the focus on top–down strategies, analyses described in this section exclude individuals ($n = 4$) who reported not explicitly trying to remember high-value items better.[2] The trial type most clearly demonstrating selective encoding is H+L−. In contrast, H+L+ trials could represent a failure to be selective, but we found no evidence for this interpretation, as no brain areas were more active during H+L− trials than during H+L+ trials. It thus seems more likely that, in terms of selectivity, H+L+ trials reflect either a successful effort to encode both items or simply good memory. Our primary contrast for examining selectivity was between H+L− and H−L+ trials, however, as both trial types yield memory for one item, but only the H+L− condition reflects successful prioritization. Analysis of differential activity between H+L− trials and H−L+ trials identified a reliable difference bilaterally in dPPC, as well as a smaller cluster in anterior left inferior frontal gyrus (Figure 4A: Table 3). These regions were more active for successful high-value memory and likely reflect neural activity associated with effective strategic memory.

The posterior parietal effect was hypothesized to reflect the role of top–down attention during successful encoding, following Uncapher et al. (2011). If so, enhanced functional connectivity between dPPC and lateral occipitotemporal cortex would be expected during successful encoding, particularly for high-value items. To test this hypothesis, connectivity analysis was used to identify regions that might be working in concert with dPPC to control memory encoding. Search space was restricted to inferior portions of lateral temporal and lateral occipital cortex, as described in Methods. A significant positive effect was found in right lateral temporal cortex when contrasting combined effects from H+L− and H+L+ trials against that from H−L− trials (Figure 4B; Table 4). The magnitude of the PPI effect shown in Figure 4B was found to be correlated with memory selectivity (the difference in the proportion of items recalled for high-value vs. low-value items), $r = .68$, $p = .010$ (Figure 4C). The total recall rate across all items was not reliably correlated with the PPI effect, $r = .37$, $p = .21$. An additional PPI activation was observed in left lateral temporal cortex

Table 4. Cluster Peaks and Relevant Subpeaks for PPI Contrast, Showing Condition-Specific Enhancement in Connectivity with a Bilateral Parietal Seed Region Defined from the H+L− > H−L+ Contrast

| Cluster Number | Region | BA | Peak MNI Coordinates | | | Z_{max} | Cluster Size (Voxels) |
			x	y	z		
Both (H+L+) or high value (H+L−) correct > neither correct (H−L−)							
1	R middle temporal gyrus	19/37	50	−56	0	3.88	190
	R inferior temporal gyrus	20/37	48	−48	−12	3.65	
	R fusiform gyrus	37	38	−54	−14	2.90	
Any item correct (H+L+, H+L−, H−L+) > neither correct (H−L−)							
1	L extrastriate visual cortex (V5/MT)	19	−40	−68	−6	3.76	129

when combining across H+L+, H+L−, and H−L− trials, relative to H−L− trials (Table 4). The magnitude of this effect showed a marginal correlation with memory selectivity, $r = .53$, $p = .065$, but no correlation with the total recall rate, $r = .03$, $p = .92$. Thus, although connectivity effects are not limited to trials in which a high-value item was successfully encoded, the overall strength of parietal–temporal connectivity during successful encoding appears to be relatively more associated with selectivity than with overall memory.

DISCUSSION

The network of brain regions exhibiting increased activity for successful memory encoding includes many familiar regions associated with directing memory effort, attention, and semantic memory. In addition, increased activity in brain regions sensitive to reward, and greater connectivity between MTL and VTA regions, was found during all types of encoding trials associated with successful subsequent memory, relative to those leading to unsuccessful memory. Thus, when anticipating the possibility of gaining an extrinsic reward, activation of the dopaminergic reward system improves memory storage in a nonselective manner.

The influence of the reward system on memory formation was not observed to be sensitive to differences between high- and low-value stimuli, although participants exhibited better memory for high-value stimuli. The most notable region to exhibit reliably greater activity when encoding high-value stimuli, relative to encoding low-value stimuli, was the dPPC. Increased activity in this region and connectivity to lateral occipitotemporal cortex were associated with selectively better memory for the high-value stimuli, suggesting the strategic direction of attention to better encode the important images. Medial posterior parietal cortex has also been described as part of a general parietal memory network, showing a distinctive pattern of deactivation at encoding and activation at retrieval (Gilmore, Nelson, & McDermott, 2015) that suggests a broad role in memory formation and retrieval. Recent studies of spatial memory have found postencoding increases in structural connectivity in precuneus, slightly ventral to this cluster, after successful encoding (Brodt et al., 2018) and increased functional connectivity between dorsal precuneus and visual cortex including occipitotemporal regions from a repeated study of spatial configurations (Schott et al., 2019). These results reinforce the idea that dPPC and its connectivity to visual regions play an important role in forming memories of spatial information. Although we cannot definitively rule out a simpler explanation of our data based on this region's role in top–down spatial attention, such as that dPPC activity during encoding reflects increased attention to spatial location, a seemingly more likely explanation combines these two perspectives. Specifically, it

follows that the parietal–occipitotemporal network is under strategic volitional control and can be selectively directed to enhance memory of important stimuli within a spatial array. This interpretation is conceptually consistent with Uncapher et al.'s (2011) proposal that dPPC activation during memory encoding serves to organize the goal-relevant subset of item information processed in lateral occipitotemporal cortex, enabling preferential encoding of that information into memory via the hippocampus.

Prior work (e.g., Gruber et al., 2016; Dillon et al., 2014; Adcock et al., 2006) has shown that increased activity in VTA and NAcc, as well as enhanced functional connectivity between MTL and VTA, is a critical mechanism strengthening memory for high-value information. Those results were observed when stimuli were presented one at a time, with cues indicating the value of each item. The central analyses were premised on contrasts created because some trials were more important than others. Thus, there was no opportunity to observe whether the reward signal produced in anticipation of encoding high-value items was capable of also strengthening memory for low-value items. This methodology additionally allows for the ambiguity that increased motivation may have led to increased attention or strategic effort on high-reward trials. Accordingly, in intentional learning paradigms, it is typically difficult to separate attention- or strategy-based mechanisms from the more direct enhancement of memory encoding via activation of the dopaminergic reward system.

Here, with high- and low-value items presented simultaneously, motivation and attentional engagement do not vary systematically across trials, and the distinct contribution of reward processing to successful memory can be seen more clearly. We observed increased activity in the reward system during memory formation regardless of whether high-value information within a trial, low-value information within a trial, or both types of information were ultimately remembered. In addition, the magnitude of increased MTL–VTA connectivity associated with successful memory formation was correlated with the total number of items recalled, regardless of the value assigned to those items. It thus appears that memory is strengthened for any stimulus presented temporally contiguous to activation of the reward system, rather than reward processing selectively strengthening memory for high-value information. These findings are consistent with past behavioral results showing enhancement for items indirectly associated with reward (e.g., Loh et al., 2016; Murayama & Kitagami, 2014) and potentially with cellular mechanisms such as synaptic tagging and capture (Redondo & Morris, 2011).

This is the first neuroimaging study to demonstrate reward-motivated use of top–down attention to enhance processing of high-value items. Prior work examining how value affects encoding strategies has focused on selective use of deep verbal encoding (e.g., Cohen et al., 2014, 2016), and we find some evidence that a similar mechanism may also be involved here. Importantly,

strategic effects of value mediated by top–down attention or verbal strategies both appear to be dissociable from effects mediated by the mesolimbic dopamine system. An alternate possibility is that reward-related activation of the dopamine system initiates the strategic direction of attention toward learning high-value items. However, this explanation would seem to predict greater reward system activity when the high-value item is successfully learned. Our finding that brain regions associated with top–down attention are more strongly activated when a high-value item, versus a low-value item, is successfully learned, whereas the reward system is activated to a similar degree whether the low-value item alone, the high-value item alone, or both items are successfully learned, argues against this possibility.

Our whole-brain analysis of subsequent memory effects (Figure 2) highlighted additional regions that contribute to encoding success, many of which broadly correspond to typical activations during successful memory (cf. Kim, 2011). These included dorsal frontoparietal areas involved in working memory and selective attention and lateral occipitotemporal areas that one would expect to be involved in processing shape stimuli. Finally, somewhat surprisingly, there was an association between activity in brain regions related to semantic processing and successful memory, despite the lack of any obvious semantic content in the images. Self-reports suggested that, in about half of our participants, some effort was made to semanticize the images. It is possible that these semantic strategies contributed to successful memory encoding, despite the abstract nature of the stimuli. Although this study is limited in its ability to address this issue, such a result would contrast with prior work suggesting that semantic representations play little role in encoding of abstract visual images (e.g., Han et al., 2011). Future work could address this issue by sorting items based on each individual's self-reports of item meaningfulness (cf. Voss, Schendan, & Paller, 2010; Voss & Paller, 2007).

Overall, these results support the hypothesis that selective enhancement of memory for information arbitrarily designated as important can be driven either by strategies or by reward processing. When both high-value and low-value information is temporally contiguous with reward anticipation, dopamine-driven reward produces better memory for both types of information. In contrast, strategy-driven engagement of top–down attention produces enhanced memory for high-value information relative to low-value information. We cannot rule out the possibility that activation of the reward system would have a greater role in memory selectivity on a delayed memory test, given prior work showing that dopamine-driven reward responses primarily enhance memory replay and consolidation (e.g., Gruber et al., 2016), and that memory enhancement assumed to be driven by that system emerges more reliably after a delay (e.g., Spaniol et al., 2014; Murayama & Kuhbandner, 2011). Still, in the data set presented here, only goal-directed strategies appeared to selectively strengthen memory for high-value information.

Beyond the theoretical implications of elucidating two distinct systems by which memory for important information is strengthened, these results also have practical implications. There are often situations in life where information that is important to learn is presented simultaneously with less-important information. Our work suggests that, in such circumstances, memory both for the important information and for irrelevant aspects of the situation are likely to be strengthened via dopamine signaling. If memory is to be optimized toward the important aspects of the situation, however, engagement of top–down attention and/or other forms of strategic encoding is likely to be necessary. These strategic mechanisms tend to require a higher degree of conscious control and also have different temporal and neural dynamics, relative to dopamine-MTL signaling. Further research will help to clarify the distinct mechanisms and complementary but overlapping roles of reward and strategy use on memory.

Notes

1.   The PPI analysis follows documentation at afni.nimh.nih. gov/CD-CorrAna and in the 3dTfitter program help file.
2.   The univariate effect in dPPC is similar when these four individuals are included. Other effects (PPI effects and the left inferior frontal gyrus univariate cluster) are not reliable in the full sample.

REFERENCES

Adcock, R. A., Thangavel, A., Whitfield-Gabrieli, S., Knutson, B., & Gabrieli, J. D. (2006). Reward-motivated learning: Mesolimbic activation precedes memory formation. *Neuron*, *50*, 507–517.

Berridge, K. C. (2007). The debate over dopamine's role in reward: the case for incentive salience. *Psychopharmacology*, *191*, 391–431.

Bethus, I., Tse, D., & Morris, R. G. (2010). Dopamine and memory: Modulation of the persistence of memory for novel hippocampal NMDA receptor-dependent paired associates. *Journal of Neuroscience*, *30*, 1610–1618.

Brodmann, K. (1909). *Vegleichende lokalisationslehre der Grosshirnde*. Leipzig, Germany: Barth.

Brodt, S., Gais, S., Beck, J., Erb, M., Scheffler, K., & Schönauer, M. (2018). Fast track to the neocortex: A memory engram in the posterior parietal cortex. *Science*, *362*, 1045–1048.

Cansino, S., Maquet, P., Dolan, R. J., & Rugg, M. D. (2002). Brain activity underlying encoding and retrieval of source memory. *Cerebral Cortex*, 12, 1048–1056.

Castel, A. D. (2008). The adaptive and strategic use of memory by older adults: Evaluative processing and value-directed remembering. In A. S. Benjamin & B. H. Ross (Eds.), *The psychology of learning and motivation* (Vol. 48). San Diego, CA: Academic Press.

Cohen, M. S., Rissman, J., Hovhannisyan, M., Castel, A. D., & Knowlton, B. J. (2017). Free recall test experience potentiates strategy-driven effects of value on memory. *Journal of Experimental Psychology: Learning, Memory, and Cognition*, 43, 1581–1601.

Cohen, M. S., Rissman, J., Suthana, N. A., Castel, A. D., & Knowlton, B. J. (2014). Value-based modulation of memory encoding involves strategic engagement of fronto-temporal semantic processing regions. *Cognitive, Affective & Behavioral Neuroscience*, 14, 578–592.

Cohen, M. S., Rissman, J., Suthana, N. A., Castel, A. D., & Knowlton, B. J. (2016). Effects of aging on value-directed modulation of semantic network activity during verbal learning. *Neuroimage*, 125, 1046–1062.

Cox, R. W. (1996). AFNI: Software for analysis and visualization of functional magnetic resonance neuroimages. *Computers and Biomedical Research*, 29, 162–173.

Craik, F. I. M., & Lockhart, R. S. (1972). Levels of processing: A framework for memory research. *Journal of Verbal Learning and Verbal Behavior*, 11, 671–684.

Craik, F. I. M., & Tulving, E. (1975). Depth of processing and the retention of words in episodic memory. *Journal of Experimental Psychology: General*, 104, 268–294.

DeWinstanley, P. A., & Bjork, E. L. (2004). Processing strategies and the generation effect: Implications for making a better reader. *Memory & Cognition*, 32, 945–955.

Di, X., Reynolds, R. C., & Biswal, B. B. (2017). Imperfect (de)convolution may introduce spurious psychophysiological interactions and how to avoid it. *Human Brain Mapping*, 38, 1723–1740.

Dillon, D. G., Dobbins, I. G., & Pizzagalli, D. A. (2014). Weak reward source memory in depression reflects blunted activation of VTA/SN and parahippocampus. *Social, Cognitive, and Affective Neuroscience*, 9, 1576–1583.

Düzel, E., Bunzeck, N., Guitart-Masip, M., & Düzel, S. (2010). NOvelty-related Motivation of Anticipation and exploration by dopamine (NOMAD): Implications for healthy aging. *Neuroscience & Biobehavioral Reviews*, 34, 660–669.

Eickhoff, S. B., Stephan, K. E., Mohlberg, H., Grefkes, C., Fink, G. R., Amunts, K., et al. (2005). A new SPM toolbox for combining probabilistic cytoarchitectonic maps and functional imaging data. *Neuroimage*, 25, 1325–1335.

Eklund, A., Nichols, T. E., & Knutsson, H. (2016). Cluster failure: Why fMRI inferences for spatial extent have inflated false-positive rates. *Proceedings of the National Academy of Sciences, U.S.A.*, 113, 7900–7905.

Friston, K. J., Buechel, C., Fink, G. R., Morris, J., Rolls, E., & Dolan, R. J. (1997). Psycho-physiological and modulatory interactions in neuroimaging. *Neuroimage*, 6, 218–229.

Geddes, M. R., Mattfeld, A. T., de los Angeles, C., Keshavan, A., & Gabrieli, J. D. E. (2018). Human aging reduces the neurobehavioral influence of motivation on episodic memory. *Neuroimage*, 171, 296–310.

Gilmore, A. W., Nelson, S. M., & McDermott, K. B. (2015). A parietal memory network revealed by multiple MRI methods. *Trends in Cognitive Sciences*, 19, 534–543.

Gruber, M. J., Gelman, B. D., & Ranganath, C. (2014). States of curiosity modulate hippocampus-dependent learning via the dopaminergic circuit. *Neuron*, 84, 486–496.

Gruber, M. J., Ritchey, M., Wang, S. F., Doss, M. K., & Ranganath, C. (2016). Post-learning hippocampal dynamics promote preferential retention of rewarding events. *Neuron*, 89, 1110–1120.

Han, S., O'Connor, A. R., Eslick, A. N., & Dobbins, I. G. (2011). The role of left ventrolateral prefrontal cortex during episodic decisions: Semantic elaboration or resolution of episodic interference? *Journal of Cognitive Neuroscience*, 24, 223–234.

Jenkinson, M., Bannister, P., Brady, M., & Smith, S. (2002). Improved optimization for the robust and accurate linear registration and motion correction of brain images. *Neuroimage*, 17, 825–841.

Jones-Gotman, M. (1986). Right hippocampal excision impairs learning and recall of a list of abstract designs. *Neuropsychologia*, 24, 659–670.

Kapur, S., Craik, F. I., Tulving, E., Wilson, A. A., Houle, S., & Brown, G. M. (1994). Neuroanatomical correlates of encoding in episodic memory: Levels of processing effect. *Proceedings of the National Academy of Sciences, U.S.A.*, 91, 2008–2011.

Kim, H. (2011). Neural activity that predicts subsequent memory and forgetting: A meta-analysis of 74 fMRI studies. *Neuroimage*, 54, 2446–2461.

Kirchhoff, B. A., & Buckner, R. L. (2006). Functional–anatomic correlates of individual differences in memory. *Neuron*, 51, 263–274.

Li, S., Cullen, W. K., Anwyl, R., & Rowan, M. J. (2003). Dopamine-dependent facilitation of LTP induction in hippocampal CA1 by exposure to spatial novelty. *Nature Neuroscience*, 6, 526–531.

Lisman, J. E., & Grace, A. A. (2005). The hippocampal-VTA loop: Controlling the entry of information into long-term memory. *Neuron*, 46, 703–713.

Lisman, J., Grace, A. A., & Düzel, E. (2011). A neoHebbian framework for episodic memory; role of dopamine-dependent late LTP. *Trends in Neurosciences*, 34, 536–547.

Loh, E., Kumaran, D., Koster, R., Berron, D., Dolan, R., & Düzel, E. (2016). Context-specific activation of hippocampus and SN/VTA by reward is related to enhanced long-term memory for embedded objects. *Neurobiology of Learning and Memory*, 134, 65–77.

Mather, M., & Schoeke, A. (2011). Positive outcomes enhance incidental learning for both younger and older adults. *Frontiers in Neuroscience*, 5, 129.

McLaren, D. G., Ries, M. L., Xu, G., & Johnson, S. C. (2012). A generalized form of context-dependent psychophysiological interactions (gPPI): A comparison to standard approaches. *Neuroimage*, 61, 1277–1286.

Milner, B. (1958). Psychological defects produced by temporal lobe excision. *Research Publications: Association for Research in Nervous and Mental Disease*, 36, 244–257.

Miotto, E. C., Savage, C. R., Evans, J. J., Wilson, B. A., Martins, M. G., Iaki, S., et al. (2006). Bilateral activation of the prefrontal cortex after strategic semantic cognitive training. *Human Brain Mapping*, 27, 288–295.

Miyashita, Y., Higuchi, S., Sakai, K., & Masui, N. (1991). Generation of fractal patterns for probing the visual memory. *Neuroscience Research*, 12, 307–311.

Murayama, K., & Kitagami, S. (2014). Consolidation power of extrinsic rewards: Reward cues enhance long-term memory for irrelevant past events. *Journal of Experimental Psychology: General*, 143, 15–20.

Murayama, K., & Kuhbandner, C. (2011). Money enhances memory consolidation—But only for boring material. *Cognition*, 119, 120–124.

Murty, V. P., Shermohammed, M., Smith, D. V., Carter, R. M., Huettel, S. A., & Adcock, R. A. (2014). Resting state networks

distinguish human ventral tegmental area from substantia nigra. *Neuroimage*, *100*, 580–589.

O'Carroll, C. M., & Morris, R. G. (2004). Heterosynaptic co-activation of glutamatergic and dopaminergic afferents is required to induce persistent long-term potentiation. *Neuropharmacology*, *47*, 324–332.

Oyarzún, J. P., Packard, P. A., de Diego-Balaguer, R., & Fuentemilla, L. (2016). Motivated encoding selectively promotes memory for future inconsequential semantically-related events. *Neurobiology of Learning and Memory*, *133*, 1–6.

Paivio, A. (1969). Mental imagery in associative learning and memory. *Psychological Review*, *76*, 241–263.

Patil, A., Murty, V. P., Dunsmoor, J. E., Phelps, E. A., & Davachi, L. (2017). Reward retroactively enhances memory consolidation for related items. *Learning & Memory*, *24*, 65–69.

Peirce, J. W. (2007). PsychoPy—Psychophysics software in Python. *Journal of Neuroscience Methods*, *162*, 8–13.

Poldrack, R. A., Mumford, J. A., Schonberg, T., Kalar, D., Barman, B., & Yarkoni, T. (2012). Discovering relations between mind, brain, and mental disorders using topic mapping. *PLoS Computational Biology*, *8*, e1002707.

Redondo, R. L., & Morris, R. G. (2011). Making memories last: The synaptic tagging and capture hypothesis. *Nature Reviews Neuroscience*, *12*, 17–30.

Schott, B. H., Wüstenberg, T., Lücke, E., Pohl, I. M., Richter, A., Seidenbecher, C. I., et al. (2019). Gradual acquisition of visuospatial associative memory representations via the dorsal precuneus. *Human Brain Mapping*, *40*, 1554–1570.

Schultz, W. (1998). Predictive reward signal of dopamine neurons. *Journal of Neurophysiology*, *80*, 1–27.

Schultz, W. (2016). Dopamine reward prediction-error signaling: A two-component response. *Nature Reviews Neuroscience*, *17*, 183–195.

Shigemune, Y., Tsukiura, T., Kambara, T., & Kawashima, R. (2014). Remembering with gains and losses: Effects of monetary reward and punishment on successful encoding activation of source memories. *Cerebral Cortex*, *24*, 1319–1331.

Shohamy, D., & Adcock, R. A. (2010). Dopamine and adaptive memory. *Trends in Cognitive Sciences*, *14*, 464–472.

Siegel, J. S., Power, J. D., Dubis, J. W., Vogel, A. C., Church, J. A., Schlaggar, B. L., et al. (2014). Statistical improvements in functional magnetic resonance imaging analyses produced by censoring high-motion data points. *Human Brain Mapping*, *35*, 1981–1996.

Slamecka, N. J., & Graf, P. (1978). The generation effect: Delineation of a phenomenon. *Journal of Experimental Psychology: Human Learning and Memory*, *4*, 592–604.

Smith, S. M. (2002). Fast robust automated brain extraction. *Human Brain Mapping*, *17*, 143–155.

Spaniol, J., Schain, C., & Bowen, H. J. (2014). Reward-enhanced memory in younger and older adults. *Journals of Gerontology: Series B*, *69*, 730–740.

Stark, C. E. L., & Squire, L. R. (2001). When zero is not zero: The problem of ambiguous baseline conditions in fMRI. *Proceedings of the National Academy of Sciences, U.S.A.*, *98*, 12760–12766.

Talairach, J., & Tournoux, P. (1988). *Co-planar stereotaxic atlas of the human brain*. New York, NY: Thieme.

Tristán-Vega, A., García-Perez, V., Aja-Fernández, S., & Westin, C. F. (2012). Efficient and robust nonlocal means denoising of MR data based on salient features matching. *Computer Methods and Programs in Biomedicine*, *105*, 131–144.

Tustison, N. J., Avants, B. B., Cook, P. A., Zheng, Y., Egan, A., Yushkevich, P. A., et al. (2010). N4ITK: Improved N3 bias correction. *IEEE Transactions on Medical Imaging*, *29*, 1310–1320.

Uncapher, M. R., Hutchinson, J. B., & Wagner, A. D. (2011). Dissociable effects of top–down and bottom–up attention during episodic encoding. *Journal of Neuroscience*, *31*, 12613–12628.

Uncapher, M. R., & Wagner, A. D. (2009). Posterior parietal cortex and episodic encoding: Insights from fMRI subsequent memory effects and dual-attention theory. *Neurobiology of Learning & Memory*, *91*, 139–154.

Van Essen, D. C., Drury, H. A., Dickson, J., Harwell, J., Hanlon, D., & Anderson, C. H. (2001). An integrated software suite for surface-based analyses of cerebral cortex. *Journal of the American Medical Informatics Association*, *8*, 443–459.

Van Essen, D. C., Glasser, M. F., Dierker, D. L., Harwell, J., & Coalson, T. (2012). Parcellations and hemispheric asymmetries of human cerebral cortex analyzed on surface-based atlases. *Cerebral Cortex*, *22*, 2241–2262.

Voss, J. L., & Paller, K. A. (2007). Neural correlates of conceptual implicit memory and their contamination of putative neural correlates of explicit memory. *Learning & Memory*, *14*, 259–267.

Voss, J. L., Schendan, H. E., & Paller, K. A. (2010). Finding meaning in novel geometric shapes influences electrophysiological correlates of repetition and dissociates perceptual and conceptual priming. *Neuroimage*, *49*, 2879–2889.

Wittmann, B. C., Schott, B. H., Guderian, S., Frey, J. U., Heinze, H. J., & Düzel, E. (2005). Reward-related fMRI activation of dopaminergic midbrain is associated with enhanced hippocampus-dependent long-term memory formation. *Neuron*, *45*, 459–467.

Wolosin, S. M., Zeithamova, D., & Preston, A. R. (2012). Reward modulation of hippocampal subfield activation during successful associative encoding and retrieval. *Journal of Cognitive Neuroscience*, *24*, 1532–1547.

Woolrich, M. (2008). Robust group analysis using outlier inference. *Neuroimage*, *41*, 286–301.

Woolrich, M. W., Ripley, B. D., Brady, J. M., & Smith, S. M. (2001). Temporal autocorrelation in univariate linear modelling of fMRI data. *Neuroimage*, *14*, 1370–1386.

Wright, A. A., Cook, R. G., Rivera, J. J., Shyan, M. R., Neiworth, J. J., & Jitsumori, M. (1990). Naming, rehearsal, and interstimulus interval effects in memory processing. *Journal of Experimental Psychology: Learning, Memory, and Cognition*, *16*, 1043–1059.

Yarkoni, T., Poldrack, R. A., Nichols, T. E., Van Essen, D. C., & Wager, T. D. (2011). Large-scale automated synthesis of human functional neuroimaging data. *Nature Methods*, *8*, 665–670.